Dimethyl Sulfoxide Containing Platinum(II) and Palladium(II) Chelate Complexes of Glyoxylic and Pyruvic Acid Thiosemicarbazones. A New Class of Cytotoxic Metal Complexes

Nicolay I. Dodoff[a], Dimitra Kovala-Demertzi[b], Maria Kubiak[c], Janina Kuduk-Jaworska[c], Andrzej Kochel[c], and Galina A. Gorneva[a]

[a] Institute of Molecular Biology, Bulgarian Academy of Sciences, Acad. G. Bonchev Street, Block 21, 1113 Sofia, Bulgaria
[b] Section of Inorganic and Analytical Chemistry, Department of Chemistry, University of Ioannina, 451 10 Ioannina, Greece
[c] Faculty of Chemistry, Wrocław University, 14 F. Joliot Curie Street, 50-383 Wrocław, Poland

Reprint requests to Dr. N. I. Dodoff. E-mail: dodoff@obzor.bio21.bas.bg

Z. Naturforsch. **61b,** 1110 – 1122 (2006); received February 14, 2006

The complexes [Pt(DMSO)(GT)] · DMSO (**1**), [Pt(DMSO)(PT)] · 1/2DMSO (**2**) and [Pd(DMSO)-(PT)] (**3**), where DMSO = dimethyl sulfoxide, H_2GT = glyoxylic acid thiosemicarbazone and H_2PT = pyruvic acid thiosemicarbazone, have been synthesized and characterized by elemental analysis, molar electric conductivity, IR, electronic and NMR (^{1}H and ^{13}C) spectra. The single crystal X-ray diffraction analysis has revealed for **1** (orthorhombic, *Pnma*, $a = 12.941(3)$, $b = 7.108(2)$, $c = 15.148(3)$ Å, $Z = 4$) that the doubly deprotonated thiosemicarbazone molecule is coordinated to Pt(II) *via* the carboxylato O, azomethine N and thiolato S atoms forming two condensed five-membered chelate rings. The fourth coordination site of Pt(II) is occupied by the S atom of DMSO. All the atoms of the complex molecule are coplanar except the methyl groups. The O atom of DMSO is in *cis*-position towards the thiolato-S atom (point group C_s). A system of hydrogen bonds of the type N–H···O links the complex molecules between them and with the lattice DMSO molecules. Similar structures have been deduced for the remaining two complexes on the basis of spectroscopic data. The three complexes and the ligand H_2GT exhibit cytotoxic activity against F4N leukemia cells, whereas the ligand H_2PT is inactive.

Key words: Palladium(II) and Platinum(II) Thiosemicarbazonato Complexes, Crystal Structure, Cytotoxic Activity

Introduction

The thiosemicarbazones (TSCs) are an object of continuous and multilateral interest not only because of their structural peculiarities and extremely rich coordination chemistry [1 – 3], but also due to their versatile pharmacological properties comprising, for instance, antimicrobial, antiviral, anticonvulsant and carcinostatic activity [4 – 6]. Special attention has been paid to TSCs derived from *N*-heterocycles with α-carbonyl groups. This class of TSCs and the corresponding metal complexes exhibit pronounced cytostatic activity [7 – 9]. Their mechanism of action consists in hindering the DNA biosynthesis, in which the inhibition of the enzyme ribonucleotide reductase plays an important role [9 – 12]. A systematic study of the coordination chemistry and cytostatic effect of Pd(II) and Pt(II) complexes of TSCs of 2-formyl- and 2-acetylpyridine derivatives was undertaken during the last decade in the laboratory of one of us (D. K.-D.) [13, 14]. Typical for these chelate complexes is the planar tridentate N,N,S-coordination of mono-deprotonated TSC ligand (Fig. 1a). Most of them exhibit *in vitro* and *in vivo* antineoplastic activity [13d, 14a – d, 15]. Such complexes, differing significantly in their structure from cisplatin and the "classical" platinum-based cytostatics [16 – 18], are expected to have a different mechanism of action, a feature which is favourable for overcoming the cisplatin resistance. Indeed, some representatives appeared to be active against cisplatin-resistant cells [14c, 15d].

Relatively less studied are platinum metal chelates with TSCs coordinating in a tridentate O,N,S-manner [19 – 21]. In continuation of our studies we undertook the synthesis of Pt(II) and Pd(II) chelates involving thiosemicarbazonato ligands with a coordi-

0932–0776 / 06 / 0900–1110 $ 06.00 © 2006 Verlag der Zeitschrift für Naturforschung, Tübingen · http://znaturforsch.com

No	Complex Formula	Analysis: found (calcd.) [%] C	H	N	Colour	Λ_m[a], Ω^{-1} mol^{-1} cm^2
1	[Pt(GT)(DMSO)] ·DMSO	17.16 (16.94)	3.16 (3.05)	8.60 (8.46)	sunflower yellow	1.09 (±0.05)
2	[Pt(PT)(DMSO)] ·1/2DMSO	17.70 (17.83)	3.22 (2.99)	8.72 (8.91)	lemon yellow	0.57 (±0.02)
3	[Pd(PT)(DMSO)]	21.63 (20.97)	3.36 (3.23)	12.13 (12.23)	orange yellow	0.66 (±0.03)

Table 1. Elemental analyses and physical properties of the complexes of H_2GT and H_2PT.

[a] Molar electric conductivity with standard deviation at 32 °C for DMSO solutions of the complexes with concentrations $0.80 \cdot 10^{-3}$, $1.02 \cdot 10^{-3}$ and $1.05 \cdot 10^{-3}$ mol l^{-1} for **1**, **2** and **3**, respectively.

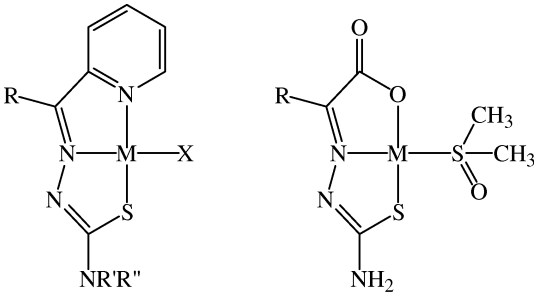

Fig. 1. Structural formulae of: a) chelate complexes of thiosemicarbazones of 2-formyl- and 2-acetylpyridine (R = H, CH_3; R', R" = H, alkyl; X = Cl, Br, monodeprotonated S-coordinated additional molecule of the ligand; M = Pd, Pt) [13, 14]; b) chelate complexes of glyoxylic acid thiosemicarbazone (H_2GT) and pyruvic acid thiosemicarbazone (H_2PT), subject of the present work: R = H, M = Pt – [Pt(DMSO)(GT)]·DMSO (**1**); R = CH_3, M = Pt – [Pt(DMSO)(PT)]·1/2DMSO (**2**); R = CH_3, M = Pd – [Pd(DMSO)(PT)] (**3**).

nated α-carboxylic group, as an attempt to design a novel group of "non-classical" cytostatic metal complexes. Such complexes should resemble the above mentioned chelates, the N atom in α-position relative to the azomethine group being replaced by another electronegative funtion, the carboxylato group. Non-ionic complexes should be formed if the fourth coordination site is occupied by an electroneutral ligand instead of a halide anion. We selected the most simple carboxylato-thiosemicarbazonato ligands, glyoxylic acid thiosemicarbazone (H_2GT) and pyruvic acid thiosemicarbazone (H_2PT), and, as a counter ligand, a dimethyl sulfoxide (DMSO) molecule (Fig. 1b). The coordination chemistry of H_2GT is still poorly studied [22], and no platinum and palladium complexes with this ligand can be found in the literature. Transition metal complexes of H_2PT in which the ligand acts as a tridentate O,N,S-chelator are well known [23–27], and among them the Cu(II) derivative has shown *in vitro* and *in vivo* antitumor activity [25a, b]. A Pt(II) chelate of H_2PT, with 1 : 2 metal-to-ligand ratio, in which the ligand is supposed to coordinate only *via* the S and O atoms, has earlier been synthesized and tested for antibacterial and antitumor activity, but neither the free ligand nor the complex have shown significant effects [28].

DMSO was considered as an appropriate fourth ligand for the following reasons. Antitumor activity has been registered for some Pt(II) complexes containing DMSO [29] and other sulfoxide ligands [30]. DMSO is a common solvent for NMR spectroscopy, as well as for biological assays, and such complexes could be conveniently studied in this coordinating solvent without the risk of changing their composition due to ligand exchange with the solvent.

Here we report the synthesis, characterization and preliminary evaluation of the cytotoxic effect of the following complexes: [Pt(DMSO)(GT)]·DMSO (**1**), [Pt(DMSO)(PT)]·1/2DMSO (**2**) and [Pd(DMSO)(PT)] (**3**) (Fig. 1b).

Results and Discussion

The complexes were synthesized by reacting the starting metal compounds (*cis*-[Pt(DMSO)$_2$Cl$_2$] or $PdCl_2$ dissolved in DMSO) with an alkalized DMSO – water solution of the corresponding thiosemicarbazone ligand, followed by recrystallization in the presence of DMSO. Analytical results and some physical properties of the complexes are listed in Table 1. The elemental analyses revealed that both Pt(II) derivatives (**1** and **2**) contain more than one molecule of DMSO *per* metal atom, and are consistent with a ratio complex species – solvate DMSO of 1 : 1 and 2 : 1, for **1** and **2**, respectively. In the Pd(II) compound (**3**), however, the ratio metal – DMSO is 1 : 1, *i. e.* it does not contain solvate DMSO molecules. All the complexes are yellow crystalline solids, soluble in DMSO and *N*,*N*-dimethylformamide, and practically insoluble in water. They are stable under usual conditions, but upon heating they decompose without melting up to 300 °C. The molar electric conductivity (Λ_m) values measured in DMSO (Table 1) are typical for non-electrolytes [31] and show that the complexes have non-ionic nature and

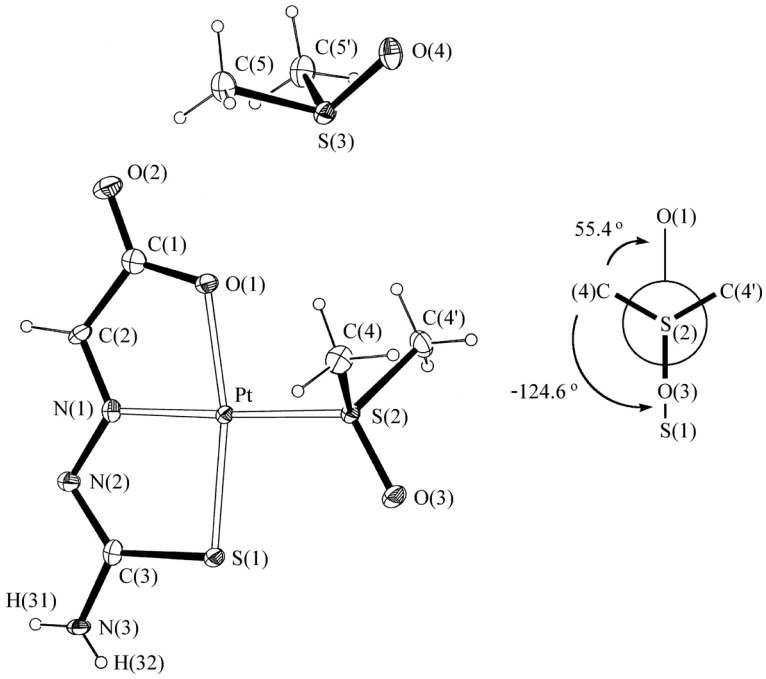

Fig 2. ORTEP drawing for the molecular structure of [Pt(DMSO)(GT)] · DMSO (**1**) with the atom labelling. Thermal ellipsoids are at 50% probability level. Insert: Newman projection along the S(2)–Pt bond.

do not undergo dissociation. Attempts to isolate the corresponding Pd(II) complex of H_2GT in an analytically pure state were unsuccessful.

Crystal structure of complex **1**

The results of the X-ray crystallography confirmed that the crystals of **1** consist of complex species [Pt(DMSO)(GT)] and solvate (lattice) DMSO molecules in a 1 : 1 ratio. The molecular structure of **1** is presented in Fig. 2, and selected geometric parameters are collected in Table 2. The doubly deprotonated H_2GT molecule is coordinated to Pt(II) *via* the carboxylato oxygen, azomethine nitrogen and thiolato sulfur atom and forms two planar condensed five-membered metalla-cycles. A sulfur-bound DMSO molecule complements the coordination tetragon of Pt(II). The S–O bond of the coordinated DMSO and the Pt–S bond of the chelate ligand are *cis*-positioned. All the atoms of the complex molecule, except the methyl groups, are coplanar; point group C_s. The geometry of the coordination node in **1** is very close to that in the bicyclic chelate Pt(II) and Pd(II) complexes of the TSCs of pyridine α-carbonyl derivatives [13, 14] mentioned above. The same could be said about the geometric parameters of the thiosemicarbazonato fragments. Thus, for instance the bond lengths Pt–O(1), Pt–N(1) and Pt–S(1) in **1** are 2.061, 1.983 and 2.252 Å, respectively, *vs.* 2.056, 1.958 and 2.253 Å for Pt–N(pyridine), Pt–N and Pt–S, respectively, in the Pt(II) complex of 2-acetyl pyridine thiosemicarbazone [14d]. X-ray crystallographic data on the free ligand H_2GT were not

Table 2. Selected bond lengths (Å), bond angles and torsion angles (deg) for **1**.

Pt–O(1)	2.061(3)	O(1)–C(1)–O(2)	124.9(4)
Pt–N(1)	1.983(3)	C(1)–O(1)–Pt	111.8(2)
Pt–S(1)	2.2517(10)	O(1)–C(1)–C(2)	115.4(3)
Pt–S(2)	2.2127(9)	C(1)–C(2)–N(1)	116.6(3)
O(1)–C(1)	1.305(5)	C(2)–C(1)–O(2)	119.7(3)
O(2)–C(1)	1.219(5)	C(2)–N(1)–N(2)	121.8(3)
C(1)–C(2)	1.515(5)	C(2)–N(1)–Pt	114.2(3)
C(2)–N(1)	1.291(5)	N(1)–N(2)–C(3)	111.3(3)
N(1)–N(2)	1.362(5)	N(2)–N(1)–Pt	124.0(2)
N(2)–C(3)	1.324(5)	N(2)–C(3)–N(3)	117.7(3)
C(3)–N(3)	1.334(5)	N(2)–C(3)–S(1)	125.5(3)
C(3)–S(1)	1.771(4)	N(3)–C(3)–S(1)	116.8(3)
O(3)–S(2)	1.477(3)	C(3)–S(1)–Pt	94.88(13)
S(2)–C(4)	1.769(3)	C(4)–S(2)–Pt	108.86(10)
O(4)–S(3)	1.506(3)	C(4)–S(2)–C(4')	102.3(2)
S(3)–C(5)	1.786(3)	C(4)–S(2)–(O3)	108.92(12)
N(1)–Pt–O(1)	81.99(12)	O(3)–S(2)–Pt	117.86(11)
N(1)–Pt–S(1)	84.35(9)	C(5)–S(3)–C(5')	96.7(2)
N(1)–Pt–S(2)	177.78(9)	C(5)–S(3)–O(4)	106.83(13)
O(1)–Pt–S(1)	166.34(8)	O(1)–Pt–S(2)–O(3)	180
O(1)–Pt–S(2)	95.79(8)	C(4)–S(2)–Pt–O(1)	55.38(11)
S(1)–Pt–S(2)	97.87(4)	C(4)–S(2)–Pt–S(1)	−124.62(11)

Table 3. Geometry of hydrogen bonding and stacking interactions of **1**[a,b,c].

D–H···A	D–H	H···A	D···A	∠D–H···A
N(3)–H(31)···O(4)[i]	0.75(5) Å	2.18(5) Å	2.889(5) Å	159(5)°
N(3)–H(32)···O(3)[ii]	0.67(5) Å	2.30(5) Å	2.953(5) Å	168(5)°

Cg1 → Cg1[iii]	Cg1 → Cg1[iv]	Cg1 → Cg2[iii]	Cg2 → Cg2[iii]	Cg2 → Pt[iii]	Distance Plane1–Plane2
3.683(1) Å	3.683(1) Å	3.992(1) Å	3.963(1) Å	3.555(1) Å	3.554(1) Å

[a] Symmetry transformations used to generate equivalent atoms: [i] $x+1, y, z$; [ii] $x+1/2, y, -z+3/2$; [iii] $x, 1+y, z$; [iv] $x, 2+y, z$; [b] Cg1 and Cg2 refer to the centroids Pt–S(1)–C(3)–N(2)–N(1) and Pt–O(1)–C(1)–C(2)–N(1), respectively; [c] Plane1 and Plane2 refer to Pt–S(1)–C(3)–N(2)–N(1)–C(2)–C(1)–O(1) and Pt[iii]–S(1)[iii]–C(3)[iii]–N(2)[iii]–N(1)[iii]–C(2)[iii]–C(1)[iii]–O(1)[iii], respectively.

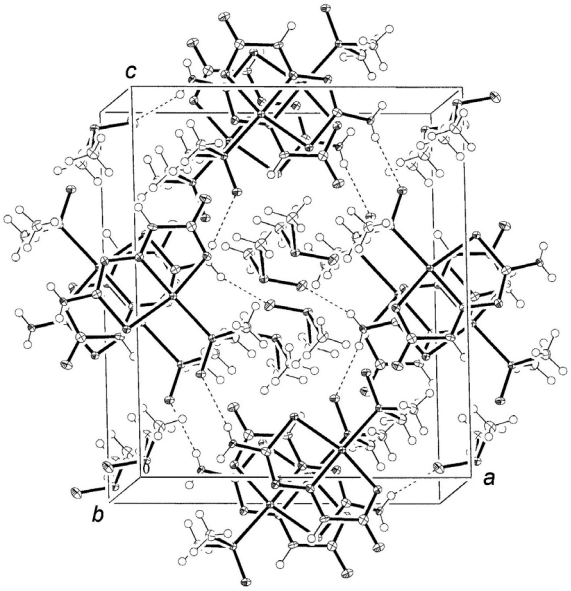

Fig. 3. View of the unit cell of [Pt(DMSO)(GT)]·DMSO (**1**) with the hydrogen bonds indicated with dashed lines.

found in the literature. A comparison is however possible with the X-ray structure data available for the crystals $H_2PT \cdot {}^1/_3H_2O$ [32]. Thus, the C(3)–S(1) bond is *ca.* 0.086 Å longer, whereas the N(2)–C(3) bond is *ca.* 0.036 Å shorter than the corresponding bond lengths in $H_2PT \cdot {}^1/_3H_2O$*, and this conforms with the expected change in bond orders in the thiolato and thione forms of a thiosemicarbazone.

Crystal structures of sulfoxide complexes of Pt(II) have been thoroughly studied by Rochon *et al.* [33], as well as by other workers [34–39]; Pd(II) sulfoxide complexes are also well characterised structurally [40–42]. The comparison shows that the bond

*In the present work pyruvic acid thiosemicarbazone was prepared as described by Timken *et al.* [24], where the compound is formulated as a hemihydrate, *i.e.* $H_2PT \cdot {}^1/_2H_2O$. In the X-ray crystallographic paper of Antosyak *et al.* [32], however, the single crystal of pyruvic acid thiosemicarbazone is assigned the composition $H_2PT \cdot {}^1/_3H_2O$.

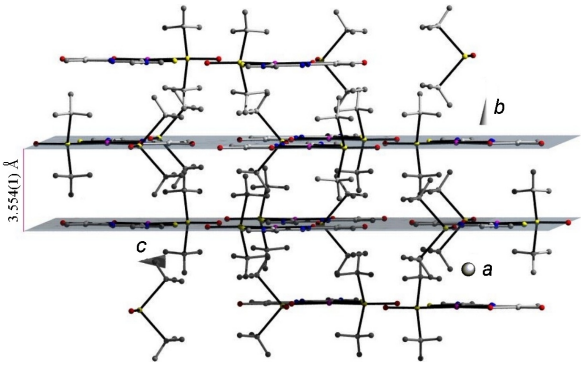

Fig. 4. View of the packing of the [Pt(DMSO)(GT)]·DMSO (**1**) molecules along the *a* axis, showing the π-π stacking interactions.

lengths and angles of the coordinated DMSO in **1** have normal values. The dihedral angle between the coordination plane and the Pt–S–O-plane varies considerably in Pt(II) sulfoxide complexes [33–39]. It seems, however, that when the sulfoxide is coordinated in *cis*-position relative to a bulky ligand, then the S–O bond lies approximately in the coordination plane [33b, c, f, 35, 36, 39]. In complex **1** the S–O bond lies exactly in the coordination plane, and the two methyl groups of DMSO are in gauche positions with respect to the Pt–O(1) bond (torsion angles O(1)–Pt–S(2)–C(4) and O(1)–Pt–S(2)–C(4'): 55.4 and −55.4°, respectively). The geometry of the non-coordinated DMSO molecule is close to that of the free crystalline DMSO [43]. The S–O bond is by 0.029 Å longer as compared to the coordinated molecule, which is a typical feature for S-coordinated DMSO [40].

The packing of the molecules of **1** is highlighted in Figs 3 and 4. The centrosymmetric unit cell contains four complex molecules and four DMSO molecules connected by a system of hydrogen bonds. The flat chelate rings are stacked in parallel planes. Two kinds of hydrogen bonds (N–H···O) are formed. The shorter bond links the amino hydrogen with the oxygen atom of a non-coordinated DMSO molecule, and the longer

Table 4. ^{1}H NMR spectroscopic data for H_2GT, $H_2PT \cdot {}^1/_2H_2O$ and their complexes.

Compound, solvent	Chemical shift (δ, ppm), multiplicity and relative intensity[a]	Assignment	Coupling constant (J, Hz) for the ^{195}Pt satellite doublet
H_2GT, DMSO-d_6	7.29 s 1H	HC=N	
	8.29 s 1H, 8.66 s 1H	NH_2	
	11.93 s 1H, 12.47 s 1H	NH, COOH	
1, DMSO-d_6	2.53 s[b]	$(CH_3)_2SO$ non-coordinated	
	3.43 ssd 6H	$(CH_3)_2SO$ coordinated	^3J(Pt–H_3C) = 16
	7.36 ssd 1H	HC=N	^3J(Pt–HC=N) = 61
	8.42 s br 2H	NH_2	
1, DMF-d_7	2.59 s 6H	$(CH_3)_2SO$ non-coordinated	
	3.54 ssd[c] 6H	$(CH_3)_2SO$ coordinated	^3J(Pt–H_3C) = 18
	7.37 ssd 1H	HC=N	^3J(Pt–HC=N) = 62
	8.55 s br 2H	NH_2	
$H_2PT \cdot {}^1/_2H_2O$, DMSO-d_6	2.07 s 3H	H_3CC=N	
	8.64 s 1H, 8.70 s 1H	NH_2	
	10.70 s 1H, 12.06 s 1H	NH, COOH	
2, DMSO-d_6	2.12 s 3H	H_3CC=N	
	2.54 s[b]	$(CH_3)_2SO$ non-coordinated	
	3.42 ssd 6H	$(CH_3)_2SO$ coordinated	^3J(Pt–H_3C) = 15
	8.22 s br 2H	NH_2	
2, DMF-d_7	2.17 ssd[d] 3H	H_3CC=N	^4J(Pt–H_3C) ≈ 6
	2.58 s 3H	$(CH_3)_2SO$ non-coordinated	
	3.52 ssd[c] 6H	$(CH_3)_2SO$ coordinated	^3J(Pt–H_3C) = 18
	8.31 s br 2H	NH_2	
3, DMSO-d_6	2.02 s 3H	H_3CC=N	
	2.54 s[b]	$(CH_3)_2SO$ non-coordinated[e]	
	7.97 s br 2H	NH_2	

[a] Notations: br – broad, s – singlet, ssd – singlet with ^{195}Pt satellite doublet; [b] inaccurate integration due to the very close position of the signal with that of the solvent; [c] the low-frequency component of the ^{195}Pt satellite doublet is partially overlapped by the signal of the water from the solvent; [d] the ^{195}Pt satellite is poorly resolved; [e] originating from the coordinated $(CH_3)_2SO$ after exchange with the solvent.

one the other amino hydrogen with the oxygen atom of a coordinated DMSO molecule. There are also π-π stacking interactions between the chelate rings with an inter-planar distance of 3.554 Å. Geometric parameters of the hydrogen bonding and stacking interactions of **1** are collected in Table 3.

NMR spectra

^{1}H NMR spectra. ^{1}H NMR spectroscopic data for the ligands and their complexes are summarized in Table 4. The spectra of H_2GT and of complex **1** in two different solvents are illustrated in Fig. 5. The assignment of the signals is based on ^{1}H NMR data of thiosemicarbazones of pyruvic acid [44] and other carbonyl compounds [45], chelate Pt(II) and Pd(II) thiosemicarbazonato complexes [13], as well as Pt(II) sulfoxide complexes [29b, 33f, 38, 46]. The assignment of the protons bound to nitrogen and oxygen was confirmed by D_2O exchange. The NH_2 protons in the spectra of the free ligands give two separate signals, as should be expected due to the restricted rotation around the H_2N–C bond. In the spectra of the complexes, however, a common broad signal appears, which suggests that upon complexation the rotational barrier about the corresponding bond decreases. A similar regularity has been described for some Hg(II) thiosemicarbazonato complexes [45a]. No signals assignable to NH and COOH protons are found in the spectra of complexes, which indicates that in all three cases the ligands act as doubly deprotonated species. The vicinal spin-spin coupling in complex **1** between the azomethine proton and the ^{195}Pt nucleus is clearly manifested (^3J(Pt–HC=N) values are 61 and 62 Hz in DMSO-d_6 and DMF-d_7, respectively). The CH_3 signal of the TSC ligand in the spectrm of **2** in DMF-d_7 shows poorly resolved ^{195}Pt satellites (^4J(Pt–H_3C) ≈ 6 Hz).

The methyl proton signals of DMSO deserve special attention. The spectra of the Pt(II) complexes **1** and **2** exhibit two kinds of DMSO signals: singlets at 2.53 – 2.59 ppm, closely situated to the signal of DMSO-d_5 of the solvent, and singlets with ^{195}Pt satellites at 3.42 – 3.54 ppm. The first kind of signals is assigned to the non-coordinate (solvate) DMSO, and the second to the coordinated DMSO. The signal at 2.53 – 2.59 ppm is so nearly positioned to the low-field side of the DMSO-d_5 quintet, that accurate integration could not be achieved (see Fig. 5). For this reason the spec-

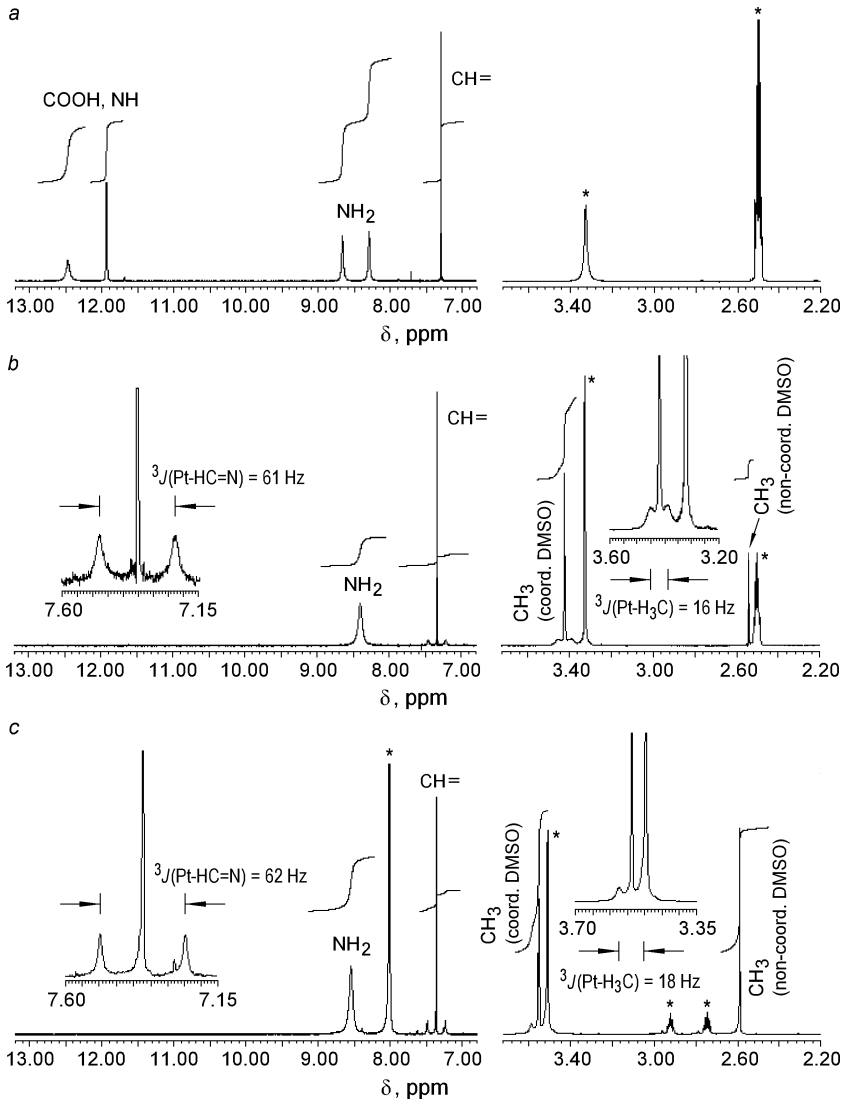

Fig. 5. ^{1}H NMR spectra (250.13 MHz) with assignments: a) H_2GT in DMSO-d_6; b) [Pt(DMSO)(GT)]·DMSO (**1**) in DMSO-d_6; c) [Pt(DMSO)-(GT)]·DMSO (**1**) in DMF-d_7. The signals due to the solvents are marked with asterisks. In the expansions the signals with ^{195}Pt satellites are shown.

tra of **1** and **2** were also recorded in DMF-d_7, and the correct integration gave 6H for the protons of non-coordinated DMSO in **1**, as required by the stoichiometry and confirmed by X-ray diffraction. In the case of **2**, the integral of the signal in question corresponds to 3H, and thus the ratio between the complex molecules and the non-coordinated DMSO is 2 : 1, in accordance with the elemental analysis. The coupling constants ^{3}J(Pt–CH_3(DMSO)) of **1** and **2** lie in the range of 15 – 18 Hz, and are by *ca.* 5 Hz smaller than the typical values for other Pt(II) DMSO complexes [29b, 33f, 38, 46]. Distinct from **1** and **2**, in the spectrum of the Pd(II) complex **3**, only one DMSO signal is observed, a singlet at 2.54 ppm. It is well known [47] that the Pd(II) complexes are kinetically much more labile than Pt(II) species. Thus, the fast exchange of the coordinated DMSO with DMSO-d_6 molecules of the solvent makes the observation of its signal impossible at ambient temperature.

^{13}C NMR spectra. ^{13}C NMR spectroscopic data for the ligands and complexes are collected in Table 5; the spectra of $H_2PT \cdot {}^{1}/_{2}H_2O$ and its complexes **2** and **3** are depicted in Fig. 6. The assignments are in agreement with the data for other chelate thiosemicarbazonato complexes [13b, d, 14d, 45] and for Pt(II) sulfoxide complexes [33f, 37]. DEPT technique was applied to

Compound	CH_3	$(CH_3)_2SO$ non-coordinated	$(CH_3)_2SO$ coordinated	C=N	COOH (COO–M)	C=S (C–S–M)
H_2GT				131.6	164.3	179.5
1		40.5	45.6	142.3	174.6	181.8
$H_2PT \cdot {}^1/_2H_2O$	12.2			138.8	164.9	179.9
2	15.0	40.4	45.6	152.5	174.0	179.0
3	15.4	40.4[a]		154.1	172.2	177.6

Table 5. ^{13}C NMR chemical shifts (δ, ppm) for DMSO-d_6 solutions of H_2GT, $H_2PT \cdot {}^1/_2H_2O$ and their complexes.

[a] Originating from the coordinated DMSO after exchange with the solvent.

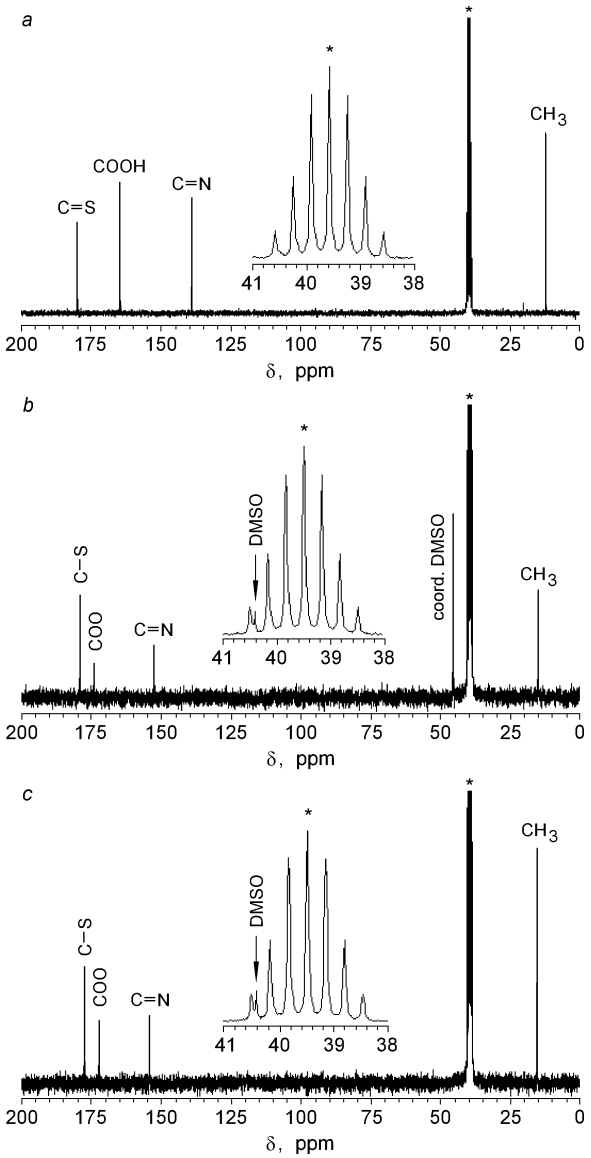

Fig. 6. $^{13}C\{H\}$ NMR spectra (62.89 MHz) in DMSO-d_6 solutions with assignments: a) $H_2PT \cdot {}^1/_2H_2O$; b) [Pt(DMSO)(PT)] $\cdot {}^1/_2$DMSO (**2**); c) [Pd(DMSO)(PT)] (**3**). The signal of the solvent, marked with asterisk, is given in the expansions. The arrows in the expansions show the signals of non-coordinated DMSO (see the text and Table 5).

confirm the assignments of the signals of CH and CH_3 carbon atoms. The signal of the coordinated DMSO appears in the spectra of the Pt(II) complexes **1** and **2** at 45.6 ppm. Such a signal was not observed in the spectrum of the Pd(II) complex **3**. The expansion of the signal of the solvent (DMSO-d_6) revealed an additional signal (at 40.5, 40.4 and 40.4 ppm for **1**, **2** and **3**, respectively) closely situated to the lowest-frequency component of the septet (Fig. 6). These signals correspond to free (non-coordinated) DMSO, and in the case of the Pt(II) complexes are due to the solvate DMSO molecules. Because of the higher kinetic lability, the coordinated DMSO in the Pd(II) complex **3** undergoes much faster exchange with the solvent, compared to the Pt(II) complexes. Thus, within the time of the NMR experiment, the coordinated DMSO is almost completely replaced by DMSO-d_6, and the liberated DMSO gives rise to the signal at 40.4 ppm. As far as the signal of the coordinatad DMSO-d_6 is concerned, its intensity should be distributed over seven lines and, under the given conditions, such a signal should easily be masked by the noise of the spectrum.

Infrared spectra

The assignment of the most important bands in the IR spectra of the ligands and their complexes is based on the data for H_2GT [19, 22] and $H_2PT \cdot {}^1/_2H_2O$ [25b, 28a, 44] and their metal complexes, chelate Pt(II) and Pd(II) complexes with tridentate thiosemicarbazonato ligands [13, 14], free DMSO [48, 49] and its complexes with Pt(II) and Pd(II) [33f, 36 – 38, 40, 46]. Selected IR spectroscopic data for H_2GT, $H_2PT \cdot {}^1/_2H_2O$ and the new complexes are presented in Table 6. The OH stretching bands of the carboxylic group in the free ligands have low intensity, appear at quite low wave numbers and are split into several components. All these features are characteristic for systems with strong hydrogen bonding [50], and have been observed by us for other compounds, too [51]. Indeed, X-ray crystallographic study of $H_2PT \cdot {}^1/_3H_2O$ crystals [32] has revealed the COOH groups to form very short H-bonds.

Table 6. Selected IR bands ($\tilde{\nu}$, cm^{-1}) for H_2GT, $H_2PT \cdot {}^1/_2H_2O$ and their complexes in CsI.

Compound					Assignment
H_2GT	**1**	$H_2PT \cdot {}^1/_2H_2O$	**2**	**3**	
		3431 m[a] 3408 s			$\nu(H_2O)$
3330 m 3288 m 3181 m	3361 m 3316 m 3234 m 3190 m	3294 m 3209 m 3135 sh	3360 sh 3321 m 3179 s	3329 m 3276 sh 3177 m	$\nu(NH_2)$, ν(NH)
3014 w	3012 w 2918 w	3003 w	3020 m 3000 m 2912 m	3019 m 2992 w 2912 w	ν(CH), $\nu(CH_3)$
2800-2400 w, br, c		2800-2400 w, br, c			ν(OH) of H-bonded COOH
1706 s		1733 s 1702 m			ν(C=O) of COOH
	1666 s		1671 s	1663 s	ν_{as}(COO) of COO–M
1636 s 1601 m 1525 s 1515 s	1648 s 1632 s 1585 w 1492 s	1626 s 1611 sh 1516 s 1488 m	1651 s 1605 m 1520 m 1497 s	1650 sh 1607 m 1522 s 1506 m	ν(C=N), $\delta(NH_2)$, δ(NH)
	1398 m		1402 m	1398 m	ν_s(COO) of COO–M
	1127 m		1122 s	1123 s	ν(SO) of coord. $(CH_3)_2SO$[b]
841 m		801 m			ν(C=S) of HN–C=S
	776 m		773 m	779 m	ν(C–S) of N=C–S–M
	414 w		415 w	420 w	ν(M–N)

[a] Notations: br – broad, c – complex, m – medium, s – strong, sh – shoulder, w – weak, δ – bending, ν – stretching; [b] see the text for an alternative assignment.

A couple of strong bands, assigned to ν_{as}(COO) and ν_s(COO), appear in the spectra of the complexes (1671 – 1663 cm^{-1} and 1402 – 1398 cm^{-1}, respectively), as should be expected for a coordinated carboxylate group [19, 22]. The thioamide band, which has considerable ν(C=S) character, undergoes a significant low-frequency shift (22 – 65 cm^{-1}) upon complexation, as it is typical for the TSC complexes containing thiolato-coordinated sulfur [13, 14, 22b]. It is known [40, 46] that compared to the free molecule, the ν(SO) stretching band of sulfur-coordinated DMSO appears at higher frequency, a typical range for Pt(II) and Pd(II) complexes being 1115 – 1150 cm^{-1} [33f, 36 – 38, 40, 46], although a value of as high as 1195 cm^{-1} has also been reported [52]. For the spectra of the new complexes the bands at 1127, 1122 and 1123 cm^{-1}, for **1**, **2** and **3**, respectively, might be assigned to ν(SO) vibrations of the sulfur-coordinated DMSO. Such an assignment is however somewhat uncertain because in the spectra of the free ligands there is also a band in this interval. An alternative assignment of these vibrations to the bands at 1180, 1153 and 1174 cm^{-1}, for **1**, **2** and **3**, respectively, should not be ruled out. In the IR spectrum of free DMSO in the solid state, the ν(SO) vibrations appear at 1037 and 1026 cm^{-1} [49a], so that the corresponding bands of the non-coordinated (solvate) DMSO in **1** and **2** should be expected near this range. Their assignment is however obstructed because of the overlapping with the rocking bands of the CH_3 groups. The bands in the range of 420 – 414 cm^{-1}, which have no corresponding band in the spectra of the free ligands, could be ascribed to metal-nitrogen stretching vibrations [13, 14]. Some other extra bands which appear in the interval of 400 – 355 cm^{-1} could tentatively be attributed to the metal-sulfur stretching vibrations (of the TSC and DMSO ligand) [13, 14, 46].

The close resemblance in the NMR as well as IR spectra of the three complexes suggests that all they share the same molecular structure pattern.

Electronic spectra

Because of solubility limitations, DMSO was the only suitable solvent for recording the spectra of the complexes in the UV and visible region. For this reason the range above 38000 cm^{-1} remained inaccessible for investigation. The electronic spectral data for the ligands and complexes are collected in Table 7. The intense bands with maxima in the interval of 34000 –

Table 7. Electronic spectral data for H_2GT, $H_2PT \cdot {}^1/_2H_2O$ and their complexes in DMSO solutions: wave numbers ($\tilde{\nu}$, cm^{-1}) and molar extinction coefficients (ε, $l\,mol^{-1}cm^{-1}$).

Compound	$\tilde{\nu}$ (ε)
H_2GT	32260 (10700)
1	30960 (14200), 25500 (500)
$H_2PT \cdot {}^1/_2H_2O$	33000 (14100), 31500 sh[a] (10800)
2	31700 (17100), 30600 sh (15100), 25500 (800)
3	34000 (16000), 28400 sh (2700), 22600 sh (140)

[a] sh – shoulder.

30600 are due to intraligand transitions, and are expected to mask some of the *d-d* bands of the metal chromophores. It is not excluded, however, that the weaker bands with maxima at 25500 cm^{-1} for **1** and **2** and at 22600 cm^{-1} for **3** are due to *d-d* transitions. If so, most probably these are transitions to the lowest-energy levels (correlating with some of the ^3E_g, $^3A_{2g}$, $^3B_{1g}$ triplets for D_{4h} symmetry), strongly influenced by spin-orbit coupling [53]. The intensity of the shoulder observed in the spectrum of **3** at 28400 cm^{-1} suggests charge-transfer or a combination of *d-d* and charge-transfer transitions [13a, 14b].

Cytotoxic effects

The sensitivity of F4N leukemia cells to the ligands and complexes was determined after 72 h incubation with the compounds. Cisplatin (*cis*-$[Pt(NH_3)_2Cl_2]$) was used as a positive control under the same conditions. The quantitative comparison of the effects of the compounds was made on the basis of the IC_{50} and EC_{50} values, representing the concentrations causing growth inhibitory and high cytotoxic cell damaging effects, respectively. The results are presented in Table 8. The effect of the free ligands differs dramatically: H_2GT inhibits very strongly the cell growth (being only twice less active than cisplatin), whereas $H_2PT \cdot {}^1/_2H_2O$ does not show any activity in concentrations up to 400 $\mu mol\,l^{-1}$. Since aldehydes are more reactive and toxic than ketones, such a difference leads us to suggest that under physiological conditions these thiosemicarbazones undergo hydrolysis to the corresponding carbonyl compounds.

All three new complexes do exhibit cytotoxic effects, but differ considerably in their activity. It should be noted that the complexes **2** and **3**, which originate from the cytostaticaly inactive ligand appeared more active than **1**, derived from the strongly active ligand. The most active is the Pt(II) complex **2**, showing an IC_{50} value *ca.* 5 times lower than that of its Pd(II) analogue **3**, and about 13 times lower than that of the platinum complex **1**. The IC_{50} value of complex **2** is roughly 7 times higher than that of cisplatin in the parallel experiment.

Table 8. Growth-inhibitory (IC_{50}[a]) and cytotoxic (EC_{50}[b]) effect of H_2GT, $H_2PT \cdot {}^1/_2H_2O$ and their complexes in F4N leukemia cells after 72 h of drug exposure.

Compound	IC_{50}, $\mu mol\,l^{-1}$	EC_{50}, $\mu mol\,l^{-1}$
H_2GT	3.0 ± 0.8	9.1 ± 1.5
1	122 ± 12	219 ± 29
$H_2PT \cdot {}^1/_2H_2O$	> 400	> 400
2	9.5 ± 2.0	16 ± 1
3	50 ± 8	143 ± 5
cis-$[Pt(NH_3)_2Cl_2]$	1.4 ± 0.6	> 10

[a] Drug concentration reducing the number of viable cells by 50%; [b] drug concentration causing the appearance of 50% dead cells.

The analysis of the growth curves revealed a significant difference between the new complexes and cisplatin. Thus, for all three complexes (as well as for the free ligands) the number of living cells progressively decreases with the compounds' concentration, whereas cisplatin shows a clear concentration interval of its cytostatic effect. The difference between highly toxic (EC_{50}) and growth inhibitory (IC_{50}) concentrations of the new complexes is about 2 – 3 times, while for cisplatin it is more than 7 times. This feature should be attributed to the presumptive difference [14c, 15] in the mechanism of cytotoxic action of the novel complexes and cisplatin. The contrast between the high cytotoxicity of complex **2** and the inactivity of the above mentioned Pt(II) bis-chelate of the same ligand [28] is noteworthy and demonstrates the importance of the structural factor.

The new class of cytotoxic DMSO containing thiosemicarbazonato complexes deserves further attention with respect to the spectrum of activity, as well as the biochemical mechanisms of action.

Experimental Section

Starting materials

K_2PtCl_4, $PdCl_2$, glyoxylic acid monohydrate, pyruvic acid, DMSO and the remaining reagents and solvents were commercial products (*purum* or *pro analysi*) used without purification. Prior to use, thiosemicarbazide was purified with charcoal and recrystallized from water. Thiosemicarbazide hydrochloride was prepared according to Timken *et al.* [24].

H_2GT was obtained from glyoxylic acid monohydrate and thiosemicarbazide in water [54, 55] with 95% yield. M. p.: 166 – 168 °C (decomp.); literature m. p.: 165 °C (decomp.) [54], 169 – 171 °C (decomp.) [55]). $H_2PT \cdot {}^1/_2H_2O$

was prepared from pyruvic acid and thiosemicarbazide hydrochloride in water [24] with 80% yield. M. p.: 189 – 190 °C (decomp.); literature m. p.: 189 °C [54].

cis-[$Pt(DMSO)_2Cl_2$] was prepared following Price *et al*. [46]: A slight excess of DMSO (molar ratio 3 : 1), dissolved in water, was mixed with a filtered aqueous solution of K_2PtCl_4, and the reaction mixture was left at r. t. overnight. The yellow needles obtained were filtered, washed with water, ethanol and diethyl ether and dried *in vacuo*. Yield: 85%. M. p.: 218 – 222 °C (decomp.). Infrared bands: ν(S=O): 1156, 1133 cm^{-1}, ν(Pt–S): 450 (sh), 431 cm^{-1}; literature: ν(S=O): 1157, 1134 cm^{-1}, ν(Pt–S): 450, 430 cm^{-1} [46].

Synthesis of the complexes

[Pt(DMSO)(GT)]·DMSO (**1**). 0.16 g (1.09 mmol) of H_2GT was dissolved in DMSO (2 ml); water (1 ml) was added, and the solution was alkalized with aqueous KOH to pH 4 – 5. This solution was added to a solution of 0.37 g (0.88 mmol) *cis*-[$Pt(DMSO)_2Cl_2$] in DMSO (3 ml); the reaction mixture was left at r. t. for 1 h, and then diluted with water to 70 ml, to produce a dark yellow precipitate. The reaction mixture was left in a refrigerator overnight; the precipitate was filtered and washed with water and ethanol to give 0.27 g (62%) of crude product which was then purified as follows. The product was dissolved in DMSO (5 ml), the solution was filtered, the filter washed with methanol (10 ml) and the solution diluted with the same solvent (total volume of methanol 21 ml). Benzene (32 ml) and *n*-hexane (45 ml) were added and the solution left in a refrigerator overnight. The precipitate was filtered and washed with ethanol and diethyl ether. The product obtained (0.21 g) was again dissolved in DMSO (4.5 ml), filtered through a sintered glass filter and the filter washed with DMSO (0.5 ml). Ethanol (14 ml) was added to the filtrate, and yellow crystals began to appear. Cyclohexane (6 ml) was added, and the solution left in a refrigerator overnight. The crystals were filtered, washed with ethanol and diethyl ether and dried *in vacuo* over P_2O_5. Final yield of recrystallized product 0.13 g (30%). Well-shaped crystals for X-ray diffraction analysis were obtained by dissolving a sample (*ca.* 0.03 g) of the recrystallized product in DMSO (1.5 ml), filtering the solution, washing the filter with DMSO (1 ml) and adding *n*-propanol (2.5 ml). The solution was left in a refrigerator, and after 1 week the yellow prismatic crystals were collected on a filter and dried as above.

[Pt(DMSO)(PT)]·1/2DMSO (**2**). 0.16 g (0.94 mmol) of $H_2PT \cdot 1/2H_2O$ was dissolved in DMSO (2.5 ml); water (1.5 ml) was added, and the pH adjusted to 5 – 6 (KOH). The solution obtained was added to a solution of 0.31 g (0.73 mmol) of *cis*-[$Pt(DMSO)_2Cl_2$] in DMSO (4 ml); the reaction mixture was left at r. t. for 0.5 h, diluted with water to 110 ml and left in a refrigerator overnight. The orange-yellow precipitate was filtered and washed with water, methanol (2 ml) and diethyl ether. Yield: 0.28 g (81%). The crude product was dissolved in DMSO (1.7 ml), the solution was filtered, and the filter washed with the same solvent (1.5 ml). Methanol (4.5 ml), diethyl ether (3 ml) and cyclohexane (2 ml) were added to the filtrate, which was left in a refrigerator for 2 days. The yellow fine needles were filtered through a sintered glass filter, washed with diethyl ether and cyclohexane and dried *in vacuo* over P_2O_5. Yield of recrystallized product: 0.17 g (49%).

[Pd(DMSO)(PT)] (**3**). 0.21 g (1.18 mmol) $PdCl_2$ was dissolved in DMSO (12 ml) upon heating (70 – 80 °C) and the solution was filtered. 0.26 g (1.53 mmol) of $H_2PT \cdot 1/2H_2O$ was dissolved in DMSO (2 ml), than water (3 ml) was added, the solution was alkalized to pH 8 – 9 (KOH) and added to the solution of $PdCl_2$ at 30 – 35 °C. After 15 min the solution was gradually diluted with water to 100 ml. The yellow precipitate obtained was filtered and washed with water, ethanol and diethyl ether. Yield: 0.35 g (86%). The product was dissolved in DMSO (7 ml) and the turbid solution was filtered through three-fold dense filter paper. The filters were washed with DMSO (10 ml) and ethanol (30 ml), then cyclohexane (15 ml) was added and the filtrate was left in a refrigerator overnight. The yellow precipitate was filtered, washed with ethanol and diethyl ether and dried *in vacuo* over P_2O_5. Yield of purified product: 0.19 g (47%). Upon heating the complexes **1** – **3** decompose, but do not melt up to 300 °C.

X-ray crystallography

The crystal of **1** was mounted on a glass fibber and flash-frozen to 100 K (Oxford Cryosystem-Cryostream Cooler). Preliminary examination and intensity data collection were carried out using a KM4-CCD diffractometer and graphite-monochromated Mo-K_α radiation generated from a diffraction X-ray tube operating at 50 kV and 35 mA. The data were corrected for Lorentz and polarization effects. Absorption corrections were performed for the intensity data ($T_{min} = 0.137$ and $T_{max} = 0.385$) [56]. The images were indexed, integrated, and scaled using the CrysAlis data reduction package [56]. The structure was solved by direct methods (SHELXS97) and refined by the full-matrix least-squares method on all F^2 data (SHELXL97) [57]. All hydrogen atoms were found in a ΔF map and were refined. Crystal data and details of data collection and refinement procedure are collected in Table 9.

Analyses and spectra

Melting points (uncorrected) were determined with a Boetius heating-plate microscope. Electric conductivities were measured at 32 °C in DMSO (Fluka, *puriss. p. a.*, $\Lambda = 1 \cdot 10^{-8} \Omega^{-1}$ cm^{-1}) using a Hydromat conductivity-meter. – The elemental analyses were performed according

Table 9. Crystal data and structure refinement for complex **1***.

Empirical formula	$C_7H_{15}N_3O_4PtS_3$
M	496.48
T [K]	100(2)
λ [Å]	0.71073
Crystal system	orthorhombic
Space group	*Pnma* (No. 62)
a [Å]	12.941(3)
b [Å]	7.108(2)
c [Å]	15.148(3)
V [Å^3]	1393.4(6)
Z	4
D_{calcd} [g cm^{-3}]	2.367
μ [mm^{-1}]	10.528
$F(000)$	944
Crystal size [mm]	$0.09 \times 0.08 \times 0.05$
θ Range for data collection [deg]	3.12 – 26.00
Limiting indices h,k,l	$-14 \le h \le 15$, $-8 \le k \le 8$, $-17 \le l \le 18$
Reflections collected	14925
Independent reflections	1479
R_{int}	0.0491
Data / parameters	1479 / 137
Goodness-of-fit (F^2)	1.159
Final R indices ($I > 2\sigma(I)$)	$R_1 = 0.0154$, $wR_2 = 0.0320$
R Indices (all data)	$R_1 = 0.0167$, $wR_2 = 0.0325$
Extinction coefficient	0.00099(7)
Largest diff. peak/hole [e.Å^{-3}]	0.733/−0.907

* Crystallographic data for the structure have been deposited with the Cambridge Crystallographic Data Centre, CCDC-293648. Copies of the data can be obtained free of charge on application to The Director, CCDC, 12 Union Road, Cambridge CB2 1EZ, UK (Fax: int. code +(1223)336-033; e-mail for inquiry: fileserv@ccdc.cam.ac.uk).

to standard microanalytical procedures (Faculty of Chemistry, St. Clement Ochridsky University of Sofia, and Faculty of Chemistry, Wrocław University). – NMR spectra were registered on a Bruker DRX-250 spectrometer operating at 250.13 MHz for the ^{1}H spectra and at 62.89 MHz for the ^{13}C{^{1}H} spectra. DMSO-d_6 and N,N-dimethylformamide-d_7 were used as solvents and tetramethylsilane as internal standard. – Infrared spectra were recorded in the solid state as CsI disks (4000 – 150 cm^{-1}) and as nujol mulls (4000 – 400 cm^{-1}) on a Bruker IFS 113 spectrophotometer, the different modes of sampling giving no significant differences. – Electronic spectra in DMSO solutions were registered using JASCO V-570 or Beckman DU-650 spectrophotometers.

Cytotoxicity studies

Mouse erythroleukemic (MEL) cells, clone F4N [58] were cultured in Dulbeco's modified Eagle medium (Gibco, Grand Island, NY) supplemented with 10% calf serum, under 5% CO_2 atmosphere at 37 °C, and passed every day at a concentration of $5 \cdot 10^5$ cells/ml. The compounds were dissolved immediately before use in DMSO to obtain stock solutions of different concentrations. The final concentration of DMSO in the medium was 1% and did not affect the cell growth. Exponentially growing cells ($0.5 \cdot 10^6$ cells/ml) were incubated in triplicate with increasing concentrations of the test compounds in 96-well microtiter plates. After 72 h of drug treatment the cells were counted haemocytometrically. The number of dead cells was determined by staining with trypan blue. The arithmetic mean and standard deviation of at least three determinations were calculated. The 50% growth inhibitory concentration (IC_{50}) was defined as the drug concentration required to reduce the number of living cells by 50%, compared to untreated control, and the 50% effective concentration (EC_{50}) – as the drug concentration causing the appearance of 50% dead cells, compared to initial amount of cells.

Acknowledgements

Thanks are due to Academician Evgeny Golovinsky for the helpful discussion. The financial support of the General Secretariat for Research and Technology at the Hellenic Ministry of Development, and the State Scholarship Foundation (IKY) is gratefully acknowledged.

[1] a) S. Padhyé, G. B. Kauffman, Coord. Chem. Rev. **63**, 127 (1985); b) D. X. West, S. B. Padhyé, P. B. Sonawane, Struct. Bonding (Berlin) **76**, 1 (1991).
[2] J. S. Casas, M. S. Garcia Tasende, J. Sordo, Coord. Chem. Rev. **209**, 197 (2000).
[3] V. M. Leovac, V. S. Jevtović, L. S. Jovanović, G. A. Bogdanović, J. Serb. Chem. Soc. **70**, 393 (2005).
[4] a) H. Beraldo, D. Gambino, Mini-Rev. Med. Chem. **4**, 31 (2004); b) H. Beraldo, Quim. Nova **27**, 461 (2004).
[5] S. N. Pandeya, S. Smitha, M. Jyoti, S. K. Sridhar, Acta Pharm. **55**, 27 (2005).
[6] B. Malawska, Curr. Topics Med. Chem. **5**, 69 (2005).
[7] A. E. Liberta, D. X. West, Bio Metals, **5**, 121 (1992).
[8] a) Y. Wang, M.-C. Liu, T.-S. Lin, A. Sartorelli, J. Med. Chem. **35**, 3667 (1992); b) M.-C. Liu, T.-S. Lin, A. C. Sartorelli, J. Med. Chem. **35**, 3672 (1992); c) M.-C. Liu, T.-S. Lin, A. C. Sartorelli, Prog. Med. Chem. **32**, 1 (1995).
[9] J. Li, L.-M. Zheng, I. King, T. W. Doyle, S.-H. Chen, Curr. Med. Chem. **8**, 121 (2001).
[10] J. C. Cory, A. H. Cory, G. Rappa, A. Lorico, M. C. Liu, T. S. Lin, A. C. Sartorelli, Adv. Enzyme Regul. **35**, 55 (1995).
[11] M. C. Miller, III, C. N. Stineman, J. R. Vance, D. X. West, I. H. Hall, Anticancer. Res. **18**, 4132 (1998).

[12] A.-M. Tsimberidou, Y. Alvarado, F. J. Giles, Expert Rev. Anticancer Ther. **2**, 437 (2002).

[13] a) D. Kovala-Demertzi, A. Domopoulou, M. Demertzis, C. P. Raptopoulou, A. Terzis, Polyhedron **13**, 1917 (1994); b) D. Kovala-Demertzi, A. Domopoulou, M. A. Demertzis, J. Valdéz-Martínez, S. Hernández-Ortega, G. Espinosa-Pérez, D. X. West, M. M. Salberg, G. A. Bain, P. D. Bloom, Polyhedron **15**, 2587 (1996); c) D. Kovala-Demertzi, M. A. Demertzis, A. Castiñeiras, D. X. West, Polyhedron **17**, 3739 (1998); d) D. Kovala-Demertzi, A. Domopoulou, M. A. Demertzis, A. Papageorgiou, D. X. West, Polyhedron **16**, 3625 (1997).

[14] a) D. Kovala-Demertzi, A. Domopoulou, M. A. Demertzis, G. Valle, A. Papageorgiou, J. Inorg. Biochem. **68**, 147 (1997); b) D. Kovala-Demertzi, J. R. Miller, N. Kourkoumelis, S. K. Hadjikakou, M. A. Demertzis, Polyhedron **18**, 1005 (1999); c) D. Kovala-Demertzi, P. N. Yadav, M. A. Demertzis, M. Coluccia, J. Inorg. Biochem. **78**, 347 (2000); d) D. Kovala-Demertzi, M. A. Demertzis, J. R. Miller, C. Papadopoulou, C. Dodorou, G. Filousis, J. Inorg. Biochem. **86**, 555 (2001); e) D. Kovala-Demertzi, M. A. Demertzis, J. R. Miller, C. S. Frampton, J. P. Jasinski, D. X. West, J. Inorg. Biochem. **92**, 137 (2002).

[15] a) A. Papageorgiou, Z. Iakovidou, D. Mourelatos, E. Mioglou, L. Boutis, A. Kotsis, D. Kovala-Demertzi, A. Domopoulou, D. X. West, M. A. Demertzis, Anticancer Res. **17**, 247 (1997); b) D. Kovala-Demertzi, M. A. Demertzis, V. Varagi, A. Papageorgiou, D. Mourelatos, E. Mioglou, Z. Iakovidou, A. Kotsis, Chemotherapy **44**, 421 (1998); c) Z. Iakovidou, A. Papageorgiou, M. A. Demertzis, E. Mioglou, D. Mourelatos, A. Kotsis, P. N. Yadav, D. Kovala-Demertzi, Anti-Cancer Drugs **12**, 65 (2002); d) D. Kovala-Demertzi, M. A. Demertzis, E. Filiou, A. A. Pantazaki, P. N. Yadav, J. R. Miller, Y. Zheng, D. A. Kyriakidis, Bio Metals **16**, 411 (2003).

[16] R. N. Bose, Mini Rev. Med. Chem. **2**, 103 (2002).

[17] V. Brabec, J. Kasparkova, Drug Resist. Updat. **5**, 147 (2002).

[18] J. Reedijk, Proc. Natl. Acad. Sci. **100**, 3611 (2003).

[19] N. V. Gerbeleu, A. V. Verezhan, O. A. Bologa, A. I. Shkurpelo, Izv. Akad. Nauk Mold. SSSR, Ser. Biol. Khim. Nauk 68 (1987); Chem. Abstr. **108**, 215239u (1988).

[20] H. A. Bayoumi, M. A. Wassel, Egypt. J. Chem. **47**, 591 (2004).

[21] a) D. Kovala-Demertzi, N. Kourkoumelis, D. X. West, J. Valdéz-Martínez, S. Hernández-Ortega, Eur. J. Inorg. Chem. 861 (1998); b) D. Kovala-Demertzi, N. Kourkoumelis, M. A. Demertzis, J. R. Miller, C. S. Frampton, J. K. Swearingen, D. X. West, Eur. J. Inorg. Chem. 727 (2000); c) P. N. Yadav, M. A. Demertzis, D. Kovala-Demertzi, A. Castiñeiras, D. X. West, Inorg. Chim. Acta **332**, 204 (2002).

[22] a) J.-L. Tian, E.-Q. Gao, Y.-T. Li, S.-X. Liu, Synth. React. Inorg. Met.-Org. Chem. **25**, 417 (1995); b) S. Liu, J. Tian, E. Gao, S. Bi, Y. Li, Synth. React. Inorg. Met.-Org. Chem. **26**, 1447 (1996); c) L. Tian, B. Zhao, Z. Zhou, Q. Yu, W. Yu, Synth. React. Inorg. Met.-Org. Chem. **32**, 939 (2002).

[23] a) A. V. Ablov, N. I. Belichuk, L. F. Chapurina, Zh. Neorg. Khim. **15**, 112 (1970); Chem. Abstr. **72**, 74158r (1970); b) A. V. Ablov, N. V. Gerbeleu, N. Ya. Negryatse, M. D. Revenko, Zh. Neorg. Khim. **15**, 123 (1970); Chem. Abstr. **72**, 74198d (1970); c) A. V. Ablov, N. V. Gerbeleu, Zh. Neorg. Khim. **15**, 1854 (1970); Chem. Abstr. **73**, 83357c (1970); d) O. A. Bologa, N. I. Belichuk, A. V. Ablov, Zh. Neorg. Khim. **23**, 1884 (1978); Chem. Abstr. **89**, 139620h (1978).

[24] M. D. Timken, S. R. Wilson, D. H. Hendrickson, Inorg. Chem. **24**, 3450 (1985).

[25] a) R. Cao, A. Garcia, E. Castell, Monatsh. Chem. **123**, 487 (1992); b) A. Diaz, R. Cao, A. Garcia, Monatsh. Chem. **125**, 823 (1994); c) A. Diaz, R. Pogni, R. Cao, R. Basosi, Inorg. Chim. Acta **275**, 552 (1998).

[26] R. Chikate, P. Sonawane, A. Khumbhar, S. Padhyé, J. R. Butcher, Inorg. Chim. Acta **205**, 59 (1993).

[27] S. Hayami, K. Hashiguchi, K. Inoue, Y. Maeda, J. Nucl. Radiochem. Sci. **5**, N1 (2004).

[28] a) N. Spassovska, R. Pelova, L. Maneva, E. Golovinsky, Pharmazie **39**, 346 (1984); b) K. Grancharov, G.-J. Krauss, N. Sopassovska, J. Miersch, L. Maneva, J. Mladenova, E. Golovinsky, Pharmazie **40**, 574 (1985).

[29] a) N. Farrell, J. Chem. Soc., Chem. Commun. 331 (1982); b) N. Farrell, D. M. Kiley, W. Schmidt, M. P. Hacker, Inorg. Chem. **29**, 397 (1990).

[30] A. Pasini, G. D'Alfonso, C. Manzotti, M. Moret, S. Spinelli, M. Valsecchi, Inorg. Chem. **33**, 4140 (1994).

[31] W. J. Geary, Coord. Chem. Rev. **7**, 81 (1971).

[32] B. Ya. Antosyak, V. N. Biyushkin, L. F. Chapurina, T. I. Malinovskii, Dokl. Akad. Nauk **327**, 219 (1992); Chem. Abstr. **118**, 113634h (1993).

[33] a) R. Melanson, F. D. Rochon, Can. J. Chem. **53**, 2371 (1975); b) R. Melanson, F. D. Rochon, Acta Crystallogr. **B33**, 3571 (1977); c) R. Melanson, F. D. Rochon, Acta Crystallogr. **B34**, 941 (1978); d) R. Melanson, F. D. Rochon, Acta Crystallogr. **B34**, 1125 (1978); e) F. D. Rochon, P. C. Kong, R. Melanson, Acta Crystallogr. **C41**, 1602 (1985); f) F. D. Rochon, J. R. L. Priqueler, Can. J. Chem. **82**, 649 (2004).

[34] F. Caruso, R. Spagna, L. Zambonelli, Acta Crystallogr. **B36**, 713 (1980).

[35] G. M. Arvanitis, C. E. Holmes, D. G. Johnson, M. Berardini, Acta Crystallogr. **C56**, 1332 (2000).

[36] G. Annibale, L. Cattalini, L. Canovese, B. Pitteri, A. Tripicchio, M. Tripicchio Camellini, M. L. Tobe, J. Chem. Soc., Dalton Trans. 1101 (1986).
[37] P. Bitha, G. O. Morton, T. S. Dunne, E. F. Delos Santos, Y. Lin, S. R. Boone, R. C. Haltiwanger, C. G. Pierpont, Inorg. Chem. **29**, 645 (1990).
[38] T. T. B. Ha, F. L. Wimmer, J.-P. Souchard, N. P. Johnson, J. Jaud, J. Chem. Soc., Dalton Trans. 1251 (1990).
[39] R. M. Dyksterhouse, B. A. Howell, P. J. Squattrito, Acta Crystallogr. **C56**, 64 (2000).
[40] M. J. Bennett, F. A. Cotton, D. L. Weaver, R. J. Williams, W. H. Watson, Acta Crystallogr. **23**, 788 (1967).
[41] D. R. Evans, M. Huang, W. M. Seganish, J. C. Fettinger, T. L. Williams, Organometallics **21**, 893 (2002).
[42] D. Tanaka, S. P. Romeril, A. G. Myers, J. Am. Chem. Soc. **127**, 10323 (2005).
[43] R. Thomas, C. B. Shoemaker, K. Eriks, Acta Crystallogr. **21**, 12 (1966).
[44] S. P. Fradkina, L. M. Kryukova, Zh. Obshch. Khim. **53**, 1904 (1983); Chem. Abstr. **99**, 211833f (1983).
[45] a) T. S. Lobana, A. Sánchez, J. S. Casas, A. Casiñeiras, J. Sordo, M. S. García-Tasende, E. M. Vázquez-López, J. Chem. Soc., Dalton Trans. 4289 (1997); b) J. S. Casas, A. Casiñeiras, M. C. Rodríguez-Argüelles, A. Sánchez, J. Sordo, A. Vázquez-López, E. M. Vázquez-López, J. Chem. Soc., Dalton Trans. 2267 (2000).
[46] J. H. Price, A. N. Williamson, R. F. Schramm, B. B. Wayland, Inorg. Chem. **11**, 1280 (1972).
[47] F. Basolo, R. G. Pearson, Mechanisms of Inorganic Reactions. A Study of Metal Complexes in Solution (Russian Edition), p. 365, Mir, Moscow (1971).
[48] G. Geiseler, G. Hanschmann, J. Mol Struct. **8**, 293 (1971).
[49] a) M.-T. Forel, M. Tranquille, Spectrochim. Acta **26A**, 1023 (1970); b) M. Tranquille, P. Labarbe, M. Fouassier, M. T. Forel, J. Mol. Struct. **8**, 273 (1971).
[50] Th. Zeegers-Huyskens, P. Huyskens, in H. Ratajczak, W. J. Orville-Thomas (eds): Molecular Interactions (Russian Edition), p. 17 – 35, Mir, Moscow (1984).
[51] a) N. I. Dodoff, Ü. Özdemir, N. Caracan, M. Ch. Georgieva, S. M. Konstantinov, M. E. Stefanova, Z. Naturforsch. **54b**, 1554 (1999); b) N. I. Dodoff, Internet J. Vibr. Spectrosc. **4**, 3, 5 (2000) [http://www.ijvs.com/volume4/edition3/section3.html].
[52] R. Romeo, S. Lanza, M. L. Tobe, Inorg. Chem. **16**, 785 (1977).
[53] A. B. P. Lever, Inorganic Electronic Spectroscopy (Russian Edition), Vol. I, p. 134, Vol II, p. 187 – 198, Mir, Moscow (1987).
[54] J. Gut, Coll. Czechoslov. Chem. Commun. **23**, 1588 (1958).
[55] Brit. 828.988 (1960); Chem. Abstr. **54**, 15412i (1960).
[56] Oxford Diffraction, CrysAlis RED, CrysAlisCCD (Version 1.171.13) and KM4CCD Oxford Diffraction Ltd., Abingdon, Oxfordshire, UK (2004).
[57] a) G. M. Sheldrick, SHELXS97, Program for the Solution of Crystal Structures, University of Goettingen (1997); b) G. M. Sheldrick, SHELXL97, Program for Refinement of Crystal Structures, University of Goettingen (1997).
[58] S. K. Dube, I. B. Pragnell, N. Kluge, G. Gaedicke, G. Steinheider, W. Ostertag, Proc. Natl. Acad. Sci. **72**, 1863 (1975).